Nanoscale Heat Transfer in the Head-Disk Interface for Heat Assisted Magnetic Recording

Haoyu Wu,[1, a)] Shaomin Xiong,[1, 2, b)] Sripathi Canchi,[2] Erhard Schreck,[2] and David Bogy[1]

[1)]*University of California at Berkeley*

[2)]*HGST, a WD company*

Laser heating has been introduced in heat-assisted magnetic recording (HAMR) in order to reduce the magnetic coercivity and enable data writing. However, the heat flow inside a couple of nanometers head-disk gap is still not well understood. An experimental stage was built for studying heat transfer in the head-disk interface (HDI) and the heat-induced instability of the HDI. A laser heating system is included to produce a heated spot on the disk at the position of the slider. A floating air bearing slider is implemented in the stage for sensing the temperature change of the slider due to the heat transfer from the disk by the use of an embedded contact sensor (ECS), and the gap between the two surfaces is controlled by the use of a thermal fly-height control (TFC) actuator. By using this system, we explore the dependency of the heat transfer on the gap spacing as well as the disk speed and temperature.

Keywords: HAMR, heat transfer, HDD

[a)]wuhaoyu@berkeley.edu

[b)]shaomin.xiong@hgst.com, xshaomin@berkeley.edu

I. INTRODUCTION

Heat Assisted Magnetic Recording (HAMR) is being pursued as one of the technologies expected to provide the increase in hard disk drive (HDD) data storage capacity required for future worldwide demands. In the HAMR system, the magnetic media is heated locally ($\sim 50\,\text{nm} \times 50\,\text{nm}$) and momentarily ($\sim 1\,\text{ns}$) to its Curie Temperature ($\sim 450\,^{\circ}\text{C}$) by a laser power source focused by a near field transducer (NFT)[1]. The designed temperature of the NFT is lower than the media's Curie Temperature for reliability. Therefore, heat flows back from the disk's heated spot to the NFT thus raising the temperature of the NFT by an unknown amount. This phenomenon is called back-heating. As the gap between the NFT and the hot media approaches a couple of nanometers, the back-heating from the hot media will be significantly enhanced and may cause an undesired temperature rise on the NFT, which could be a reliability issue for the entire HAMR system.

Therefore, it becomes vital to understand the heat transfer between two surfaces with nanoscale separations. A few theoretical models have been proposed and some experiments have been performed to verify the models[2–10]. Chen et al.[2] used an air bearing cooling model to predict the heat transport and the temperature distribution on the slider surface. This model holds for most cases when the temperature difference is around or less than $100\,\text{K}$ and has been used for several different applications in the past ten years[3–5]. However, this model only takes air conduction into account and may become less applicable when a significant amount of radiation and conduction occurs. Narayanaswamy and Chen[6] set up a radiative heat transfer model between two spheres and corresponding experiments were performed[7]. However, the model is only examined for gaps greater than $30\,\text{nm}$. Recently, Budaev and Bogy[8–10] established a phonon tunneling model to predict nanoscale heat transport. They pointed out that the correlations between two surfaces cannot be neglected when the distance between the two surfaces is within the range of the radiation's wavelength, and therefore it may contribute to the heat transport.

In this paper, we introduce a stage that was built to systematically study the heat transfer between two flat surfaces that are a few nanometers apart by implementing the localized temperature sensing capability and the nanometer gap control technology existing in current advanced HDD systems.

The paper is organized as follows. In Section II, the basic principle of the experimental
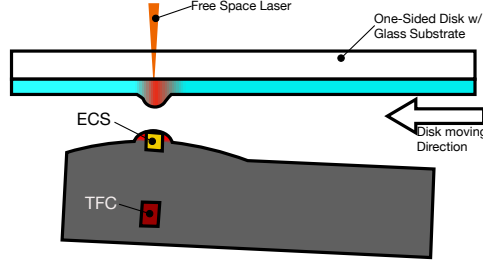
FIG. 1: The diagram shows the back-heating experiment. The head is flying on the one-side disk. The ECS and the TFC are explicitly shown but other components are omitted. The free space laser is illuminating from the back of the disk and focusing on the metal side.

setup and the experimental procedure are discussed, including the means of establishing a nanoscale gap and the temperature difference between the two surfaces. The temperature calibration and the back-heating experiment are explained. In Section III, the experimental data is analyzed and the results are presented. The paper is concluded in Section IV.

II. SYSTEM SETUP AND EXPERIMENTAL PROCEDURE

The key to observing the nanoscale heat transfer is to create two surfaces that are separated by a nanoscale gap of vacuum or gas. This can be achieved by the mechanism of the HDD recording head flying above the rotating disk. Conventionally, the gap between the head and the disk, or head-disk clearance (d_{HD}), can be maintained in a range of several nanometers with a modern production head. Moreover, d_{HD} can be adjusted if the head is equipped with a thermal fly-height control (TFC) system[11]. The head and the disk will be in contact if $d_{HD} = 0\,\mathrm{nm}$. The approximate position of the TFC element in the head is shown in Fig. 1. The TFC element is a resistor that can induce Joule heating when it is supplied with electric current. The Joule heat then produces the thermal deformation in the slider of the head, causing a protrusion on the slider's air bearing surface (ABS), and finally adjusting d_{HD}. By controlling the TFC, d_{HD} can be actively controlled in the range of $0\,\mathrm{nm}$ to $15\,\mathrm{nm}$.

Heat flow occurs when there is a temperature difference between the two surfaces, and a larger temperature difference makes the heat flux more pronounced. In our approach, a free space laser focused on a one-side coated glass disk is used to achieve this goal, as shown in

Fig. 1. One side of the disk is coated with a 100 nm thick metal layer (front side). Then a carbon overcoat and lubricant are deposited on this side to ensure flyability[12,13]. The other side of the disk (back side) is left with no further processing. A free space laser light is illuminated from the back side of the disk, passing through the glass substrate and focusing on the front side layer. The wavelength of the laser is 780 nm. The metal layer of the disk is thick enough to ensure that no laser light leaks through the layer. Although the laser heating spot is on the order of a few microns in our experiment, which is much larger than the heated spot in the real HAMR system, the heat transfer mechanism in our experiment and the HAMR system should be the same, regardless of the size of the heated spot as long as the heated area is much larger than the gap. In that case the heat transfer configuration can be modeled by two flat plats separated by a constant gap. In fact, such a micron sized heating spot is beneficial for studying the mechanism as the temperature profile is more uniform across the temperature sensing location.

The temperatures of both surfaces are experimentally calibrated. The disk is heated by the free space laser allowing the temperature of the disk surface (T_D) to be controlled by applying different laser powers (P_L). It has been shown that the peak temperature rise on the rotating disk surface is linearly proportional to the P_L[14,15].

As a consequence, this linear relationship can be easily calibrated by using a thin phase change film the microstructure of which changes when the phase change temperature is reached.

A glass disk coated with such a 20 nm phase change material (PCM) was used for the calibration, with a phase change temperature (T_{PC}) at 300 °C[16]. The laser was focused to the metal surface through the disk's glass back side at the room temperature of 25 °C. The topography of the phase change material also starts to change as T_D approaches T_{PC}. The topography change can be measured by an atomic force microscope (AFM). Fig. 2a shows the disk temperature calibration results. It can be seen that phase change shows at the P_L of 275 mW. This calibration indicates that the equivalent T_D will increase by 1 K when P_L increases by 1 mW.

The temperature of the head is measured by an embedded contact sensor (ECS)[17], which is a temperature sensitive resistor. It is embedded on the surface of the slider as shown in Fig. 1. The ECS was originally designed to be used to detect head-disk contact by sensing the cooling effect and frictional heating. In this study, it serves as a temperature indicator
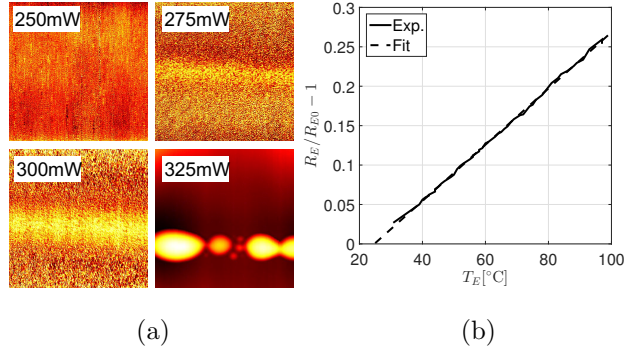
FIG. 2: (a) shows the AFM images of the phase change disk after laser heating. (b) shows the calibration curve for the ECS. The solid line is the experimental curve and the dash line is the fitted curve.

for the ABS. The relation between the resistance of the ECS and its temperature is

$$R_E(T_E) = R_{E0}(1 + \alpha_{T_0}(T_E - T_0)),$$ (1)

where $R_E(\theta_E)$ and R_{E0} are resistances of the ECS at any ECS temperature T_E and room temperature T_0, and α_{T_0} is the temperature coefficient of resistance at T_0. α_{T_0} was calibrated in an isolated environmental oven. An ohmmeter and a thermometer were used to measure the resistance of the ECS and the environment temperature simultaneously. The result of this calibration is shown in Fig. 2b. A linear regression of the measurement yields the temperature coefficient value is $3.5 \times 10^{-3}\,\mathrm{K}^{-1}$.

The TFC power is applied for d_{HD} control. The TFC heater inside the head also raises the temperature of the slider and the ECS senses this temperature rise as well. In other words, the ECS is heated by the TFC in the head which is referred to as "TFC-heating", and by the heat flow from the hot media which is called "back-heating". Or,

$$\theta_E = \theta_E^L + \theta_E^T,$$ (2)

where θ_E is the total temperature increase of the ECS from T_0. The superscripts $\cdot^L$ and $\cdot^T$ indicate that the temperature change is caused by the laser or the TFC, respectively. In the experiment, θ_E can be acquired by ECS measurements with the laser turned on for a fixed TFC power (P_T). On the other hand, θ_E^T can be acquired with the laser turned off for the same P_T. And the difference is the portion of the temperature rise caused solely by the laser heating of the disk.

With head and disk temperature calibration data available, the back-heating experiment can be done. As discussed above, a beam of laser illuminates the back of the disk with the beam size in microns. As the disk is rotating and the head is flying on the disk, the position of the laser beam is adjusted such that the ECS on the ABS is positioned directly above the heated spot on the disk. This also gives the maximum temperature increase of the ECS. The temperature of the ECS increases due to the heat transfer between the disk and the ABS. When this setup is completed, only the P_L (or equivalently disk temperature T_D) and P_T will change. Therefore, Eq. (2) leads to

$$\theta_E^L = \theta_E(T_D, P_T) - \theta_E^T(P_T) = \theta_E^L(T_D, P_T). \tag{3}$$

It is to be noticed that θ_E^T is a function of only P_T, because the θ_E^T represents the ECS temperature rise solely caused by the TFC when there is no laser power, i.e., $P_L = 0\,\mathrm{mW}$. So θ_E^L is a function of T_D and P_T.

During the experiment, the laser was adjusted initially to a certain power and remained fixed during one set of experiments. For each value of laser power, the voltage of the TFC was controlled as a ramp function. The acoustic emission (AE) signal was monitored to detect the head-disk contact[18,19]. In this way the resistance of the ECS (R_E) was acquired.

When the laser was turned off, the ECS was only heated by the TFC and θ_E^T can be acquired. When the laser was at non-zero power, then θ_E was achieved. θ_E^L can be calculated accordingly by Eq. (3).

III.   RESULTS AND ANALYSIS

The ECS temperature increase, θ_E, is plotted in Fig. 3a versus the TFC power, P_T, for different fixed values of the laser power, P_L, where P_L was set to $0\,\mathrm{mW}$ and $75\,\mathrm{mW}$ to $400\,\mathrm{mW}$. The corresponding values of the disk temperature, T_D, are indicated at the end of each curve. The curve with the dashed line corresponds to $P_L = 0\,\mathrm{mW}$, representing the ECS temperature increase caused by the TFC, $\theta_E^T(P_T)$, which is called the TFC-heating curve. The other curves represent the total ECS temperature increase, $\theta_E(T_D, P_T)$, which are called back-heating curves. In Fig. 3a, each curve has a start and an end. The curve starts when the head is at the passive flying status or initial state. It is marked by 'o', at which point $P_T = 0\,\mathrm{mW}$. The curve ends when there is a head-disk contact. The corresponding
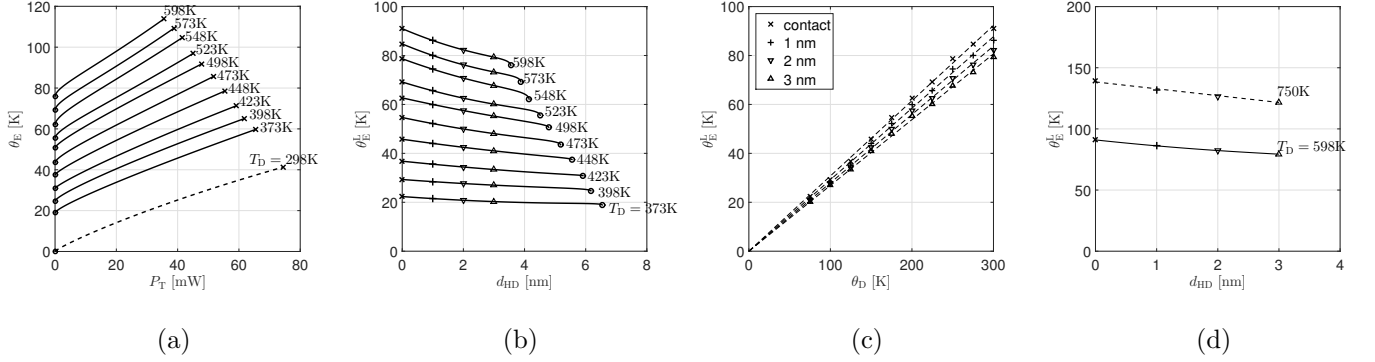
FIG. 3: Experimental Results and Analysis. (a) shows the ECS temperature increase as a function of the TFC power for fixed values of the laser power. The different curves represent different laser powers or equivalently disk temperatures as indicated at the end of each curve. (b) shows the result of subtraction. Different curves represent different laser powers or equivalently disk temperatures. (c) shows the relationship between the disk temperature and the ECS temperature. Different curves represent different clearance profiles. (d) shows the prediction of the ECS temperature when the disk reaches Curie Temperature.

TFC power is called contact power (P_C). This is marked by 'x'. It can be seen that P_C decreases as T_D increases. This is because the laser heating causes a local thermal bump on the disk at the position of the slider. The disk bump acts similar to the TFC-induced slider protrusion to reduce the fly height, which lowers the initial passive d_{HD}, resulting in the decrease of P_C.

θ_E^L can be calculated according to Eq. (3), by subtracting the TFC-heating curve from the back-heating curves. Also, the back-off method[4] is used to calculate d_{HD}. $d_{HD} = 0\,\text{nm}$ when $P_T = P_C$ and increases by $0.1\,\text{nm}$ per $1\,\text{mW}$ decrease of P_T. Fig. 3b shows the results of the data processing. Notice that θ_E^L is plotted in reverse order, being shown as a function of d_{HD}, at each fixed value of T_D.

In Fig. 3c, several points of each curve are extracted from Fig. 3b and plotted with respect to disk temperature increase θ_D. These points include the contact points and points with $d_{HD} = 1\,\text{nm}$, $2\,\text{nm}$ and $3\,\text{nm}$. It is clear that the θ_E^L values at these three states are proportional to θ_D.

The head-disk temperature rise ratio (η) is defined as

$$\eta = \frac{\theta_E^L}{\theta_D}. \tag{4}$$

Therefore, with linear regressions, η_0, η_1, η_2 and η_3 are 0.308, 0.292, 0.280 and 0.269 respectively, where η_x stands for η with $d_{HD} = x\,nm$. The reason of $\eta_0 > \eta_1 > \eta_2 > \eta_3$ is because a smaller gap between the head and the disk produces a larger heat transfer coefficient, causing more heat to be transferred from the disk back to the head.

The disk temperature in the experiment was restricted to the range of $298\,\mathrm{K}$ to $553\,\mathrm{K}$. However, the operating temperature in HAMR system is $\sim 750\,\mathrm{K}$. Since there is no explicit non-linear effect in the system, linearity can be assumed for extrapolation.

If $\theta_D = 452\,\mathrm{K}$ is substituted into to Eq. (4), we can conclude that if the free space laser were to heat the disk to its Curie Temperature, the corresponding temperature rise on the ECS would be $139\,\mathrm{K}$, $132\,\mathrm{K}$, $127\,\mathrm{K}$ and $122\,\mathrm{K}$ when $d_{HD} = 0\,\mathrm{nm}$, $1\,\mathrm{nm}$, $2\,\mathrm{nm}$ and $3\,\mathrm{nm}$ respectively, and θ_E^L increase rate with respect to d_{HD} decrease is $5.6\,\mathrm{K/nm}$ based on the linear regression as shown in Fig. 3d as the dash line. This is a very high back-heating temperature[20]. Clearly the temperature increase is a function of the gap distance between the head and the disk. This implies that the heat transfer model has to be a strong function of the gap. Recent results in thermal modeling in references[4,8–10] show such a dependence. More modeling still needs to be done for the head-disk interface to get a better prediction of NFT back-heating, but this experiment indicates the back-heating is significant for nanoscale gaps when the disk is at the Curie Temperature in HAMR systems.

IV. SUMMARY AND FUTURE WORK

In this paper, a nanoscale heat transfer experiment is reported based on the current HDD design. The key of the study relies on the fact that the gap between the head and the disk is in the scale of $\sim 10\,\mathrm{nm}$. The study shows that the temperature increase of the heated slider surface is a linear function the temperature rise of the heated disk surface. It also shows that the protrusion on the disk significantly decreases the passive flying height. This study is an indicator of how strong the heat transfer is in a nanoscale gap. In the future, further modeling studies will be done to compare with the experimental result to validate different nanoscale heat transfer models.

ACKNOWLEDGMENTS

REFERENCES

[1] M. H. Kryder, E. C. Gage, T. W. McDaniel, W. A. Challener, R. E. Rottmayer, G. Ju, Y.-T. Hsia, and M. F. Erden, Proceedings of the IEEE **96**, 1810 (2008).

[2] L. Chen, D. B. Bogy, and B. Strom, IEEE Transactions on Magnetics **36**, 2486 (2000).

[3] J. Zheng, D. B. Bogy, S. Zhang, and W. Yan, Tribology letters **40**, 295 (2010).

[4] J.-Y. Juang and D. B. Bogy, Journal of Tribology (Transactions of the ASME) **129**, 570 (2007).

[5] J. Xu, Y. Shimizu, M. Furukawa, J. Li, Y. Sano, T. Shiramatsu, Y. Aoki, H. Matsumoto, K. Kuroki, and H. Kohira, IEEE Transactions on Magnetics **50**, 114 (2014).

[6] A. Narayanaswamy and G. Chen, Physical Review B **77**, 075125 (2008).

[7] S. Shen, A. Narayanaswamy, and G. Chen, Nano Letters **9**, 2909 (2009).

[8] B. V. Budaev and D. B. Bogy, Applied Physics Letters **104**, 061109 (2014).

[9] B. V. Budaev and D. B. Bogy, Journal of Applied Physics **117**, 104512 (2015).

[10] B. V. Budaev and D. B. Bogy, Zeitschrift für angewandte Mathematik und Physik , 1 (2015).

[11] K. Aoki, T. Hoshino, T. Iwase, T. Imamura, and K. Aruga, Magnetics, IEEE Transactions on **41**, 3043 (2005).

[12] H. Wu, A. R. Mendez, S. Xiong, and D. B. Bogy, Journal of Applied Physics **117**, 17E310 (2015).

[13] S. Xiong, H. Wu, and D. Bogy, in *SPIE Optical Engineering+ Applications* (International Society for Optics and Photonics, 2014) pp. 920109–920109.

[14] S. Xiong and D. B. Bogy, IEEE Transactions on Magnetics **50**, 1 (2014).

[15] N. Tagawa, H. Tani, and K. Ueda, Tribology letters **44**, 81 (2011).

[16] I.-H. Chao, L. Pan, C. Sun, X. Zhang, and A. S. Lavine, Journal of Micro and Nano-Manufacturing **2**, 031003 (2014).

[17]Y. Shimizu, J. Xu, H. Kohira, M. Kurita, T. Shiramatsu, and M. Furukawa, IEEE Transactions on Magnetics **47**, 3426 (2011).

[18]Y.-K. Chen, J. Zheng, and D. B. Bogy, Applied Physics Letters **100**, 243104 (2012).

[19]Y.-K. Chen, A. N. Murthy, R. Pit, and D. B. Bogy, Tribology letters **54**, 273 (2014).

[20]N. Zhou, L. M. Traverso, and X. Xu, Nanotechnology **26**, 1 (2015).